Engineering Geology 200 (2016) 31–46

Contents lists available at ScienceDirect

Engineering Geology

journal homepage: www.elsevier.com/locate/enggeo

Tunnel boring machine collision with an ancient boulder beach during the excavation of the Barcelona city subway L10 line: A case of adverse geology and resulting engineering solutions

Marta Filbà [a], Josep Maria Salvany [b,*], Jordi Jubany [c], Laura Carrasco [c]

[a] Getinsa-Payma S.L., Avda. Cerdanyola 92-94, 08174 Sant Cugat del Vallés, Barcelona, Spain
[b] Dept. d'Enginyeria del Terreny, Cartogràfica I Geofísica, Universitat Politècnica de Catalunya, Jordi Girona 31, D2, 08034 Barcelona, Spain
[c] Dept. de Política Territorial i Obres Públiques, Generalitat de Catalunya, Josep Tarradellas 2-6, 08029 Barcelona, Spain

ARTICLE INFO

Article history:
Received 5 February 2015
Received in revised form 18 November 2015
Accepted 25 November 2015
Available online 27 November 2015

Keywords:
Barcelona
Subway L10 line
Tunnel boring machine
Jet grouting
Holocene delta
Boulder beach

ABSTRACT

The existence of a layer of hard boulders up to 1 m in size within the soft sediments of the Holocene Llobregat delta in the SW of Barcelona city caused the damage and stoppage of the EPB-type tunnel boring machine that excavated the subway L10 line. This layer constitutes a detrital deposit of exceptionally large grain size developed in the base of the delta. It originated as an alluvial fan in the northern margin of the delta during the last fall of the Mediterranean Sea level, at the end of the Pleistocene period. The subsequent sea level rise (Holocene transgression) caused the flooding of this alluvial fan and the reworking of its materials by sea waves. Thereby a retrogradant boulder beach developed, in which the largest rock fragments of the former alluvial fan remained densely packed. The tunnel boring machine precisely collided with the main boulder concentration area of this ancient beach. The cutter tools and the structure of the cutterhead were seriously affected. The repair tasks required the excavation of a mine in the tunnel face under atmospheric pressure and a sealing and stable environment. To get these conditions a jet grouting block from the surface was performed to consolidate the deltaic sediments around the tunnel face. Additional TAM injections were carried out to improve some deficiencies in the sealing of the block. Subsequently the shield of the tunnel boring machine was embedded into the block and the water table was depressed by pumping wells. After 13 months of complicated works, the tunnel boring machine resumed the excavation encountering further problems. Although the layer of boulders was early identified by the geological and geotechnical studies of the L10 constructive project, its precise geological characteristics and potential adverse influence on tunnelling was then not valued in depth. A better knowledge of the geology of this layer would have been helpful in order to foresee the incident and propose alternatives.

1. Introduction

During the excavation of the Barcelona subway L10 line through the soft sediments of the Llobregat delta (Fig. 1), the tunnel boring machine collided with a layer of hard boulders, up to 1 m in size. The EPB-type tunnel boring machine (Maidl et al., 1996) used was designed to excavate soft grounds and was not able to cross this layer, which caused its damage and stoppage. The engineering tasks to repair and restart the machine lasted for 13 months causing an important delay and overcost of the tunnel construction.

The geology, hydrogeology and geotechnical characteristics of the L10 line, as well as those of the L9 line (both constructed at the same time), were studied in detail in the constructive project (GISA, 2002). Additional specific studies were carried out in certain areas in order to improve the knowledge on the subsoil materials to prevent problems during the construction of the tunnel (Bono et al., 2008; Cabrera et al., 2009; Filbà, 2007; Font-Capó et al., 2011, 2015; Martí et al., 2008; Mignini et al., 2008; Orfila et al., 2007). The layer of boulders was detected at the constructive project phase. However, it was underestimated as a potential cause of problems and no specific studies were performed for this case. It was assumed that boulders would probably be disperse and would not be an insuperable obstacle for the tunnel boring machine.

The onset of problems encountered by tunnel boring machines due to adverse geology is a subject that has been treated in many studies for quite a long time (Deere, 1981). The studies describe a wide variety of geological conditions that can be an obstacle to the progress of this type of machines. The most frequent cases being the jamming and stoppages of tunnel boring machines due to squeezing grounds (Bilgin and Algan, 2012; Farrokh and Rostami, 2009; Ma and Wang, 2014; Ramoni and Anagnostou, 2010), infillings of karstic cavities (Filipponi and Ganguly, 2012; Kolic et al., 2009; Zarei et al., 2012), residual tectonic

* Corresponding author.
E-mail addresses: mfilba@getinsapayma.com (M. Filbà), josepm.salvany@upc.edu (J.M. Salvany), jordi.jubany@gencat.cat (J. Jubany), laura.carrasco@gencat.cat (L. Carrasco).

http://dx.doi.org/10.1016/j.enggeo.2015.11.010
0013-7952/

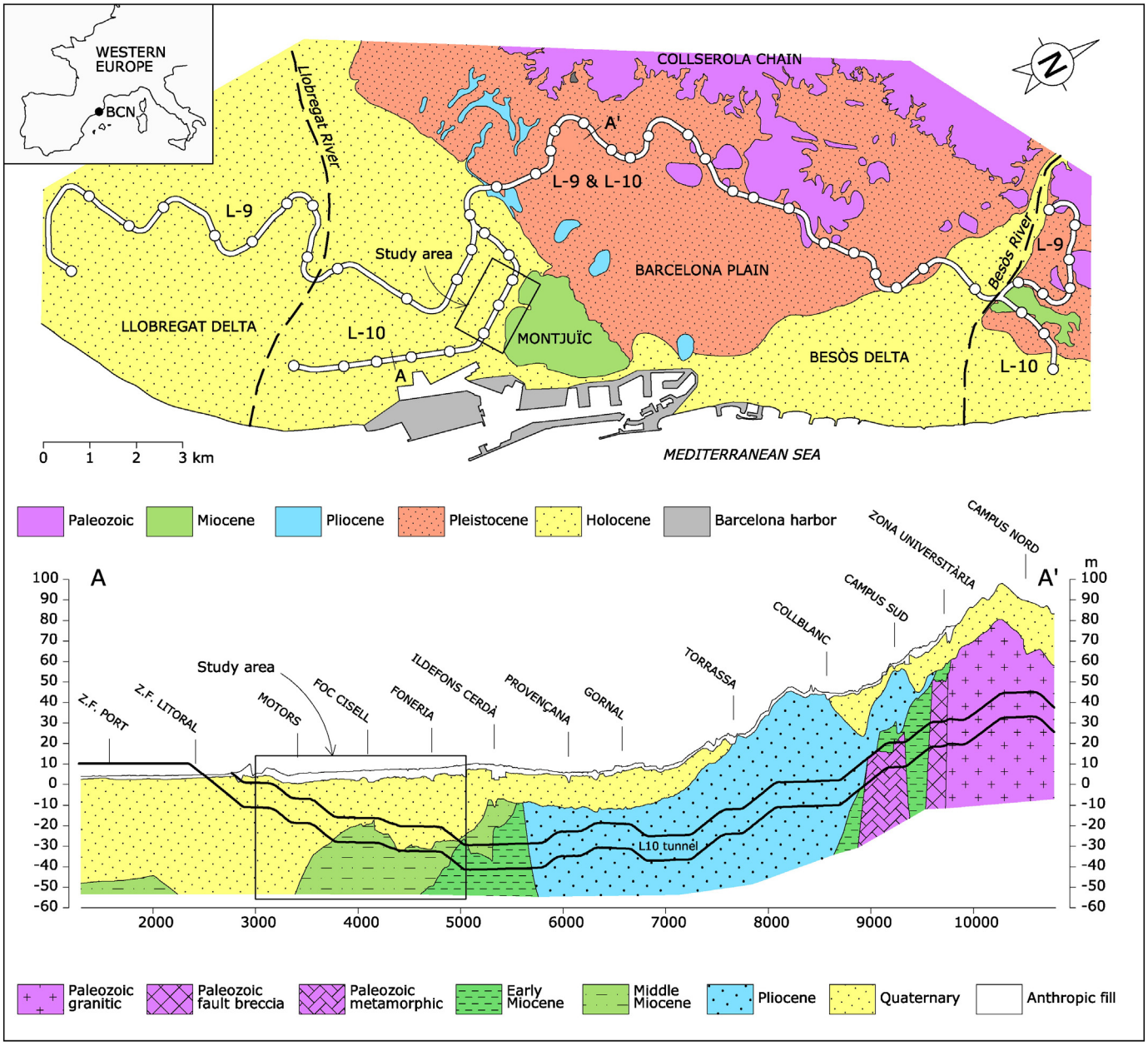

Fig. 1. Upper part: geological map of L9 and L10 lines through the Barcelona plain and the Llobegrat and Besòs deltas. Lower part: geological cross-section of L10 line between the Barcelona harbour and the Collserola chain (adapted from GISA, 2002).

stresses (Shang et al., 2004), and groundwater or gas inflows (Babendererde, 2003; Day, 2004; Tseng et al., 2001; Shahriar et al., 2009; Wenner and Wannenmacher, 2009). Frequently, some of these geological adversities can occur at the same time during the excavation of a same tunnel (Grandori et al., 1995; Shang et al., 2004). Such problems become especially complicated to resolve when they occur in urban areas (Guglielmetti et al., 2008; Kovári and Ramoni, 2006; Marchionni and Guglielmetti, 2007).

In order to provide new insights in the field of mechanized tunnelling, the present paper describes the damages occurred in the cutterhead of the tunnel boring machine because of the layer of boulders and the adopted solutions to repair and restart it in a complicated urban context. The paper also describes the geological characteristics and origin of this layer of boulders, known in detail after the tunnel construction, and how this knowledge might have been useful to prevent or minimize the tunnelling problems.

2. General description of the L9–L10 subway project

The L9 and L10 lines are two branches of the same Barcelona subway project, which was promoted by the Catalonian Government (Generalitat de Catalunya) in the year 2001 with approval of the 2001–2010 Infrastructure Master Plan. They constitute two perimetral lines designed to connect areas that still have no subway service in the northern part of Barcelona city and the neighbouring populated areas in the Besòs and Llobregat deltas. Moreover, the lines maximize the existing subway network with the construction of powerful intermodal transportation hubs. The construction of these lines started to develop during the year 2002. Between the years 2009 and 2011 a total of 11 km and 12 stations of the northern part of the project were open to the public service. At present, the works will complete the section of the L9 line between the airport and the university campus of Barcelona, with the opening of 20 additional kilometres and 15 new stations,

which are expected to be ended in 2016. There is no specific date for the completion of the project.

Both lines sum a total length of 50 km. Most of the lines (43.7 km) run underground, while the rest runs in the surface by a viaduct. In its central part, both lines run together following a single tunnel that crosses the highest part of Barcelona, along the SE slope foot of the Collserola chain (Fig. 1). To the south, the two lines end up separating. L9 crosses the Llobregat delta plain and goes to the Barcelona airport, while L10 follows the northern margin of the delta towards the Barcelona harbour and the Zona Franca industrial park. To the north, both lines also separate and finalize at different points of the Besòs delta. As a hole, both lines constitute the biggest Barcelona subway line constructed until now. They connect 5 neighbouring cities of the metropolitan area of Barcelona, the airport, the harbour and the high-speed train (AVE).

The lines cross dense urban areas below narrow streets and abundant preexisting underground structures, as well as through heterogeneous soils with extremely variable geological and geotechnical characteristics. Moreover, the underground water table normally remains above the tunnel crown. These aspects led to consider the excavation of the L9 and L10 lines using tunnel boring machines as the best method to guarantee safety and optimize the planning work.

The so-called "L9 solution" consisted in the excavation of a tunnel of large diameter (12 m in the main part of the route) with an intermediate slab that separates the tunnel in two halves where the to and fro trains circulate on two different levels (Schwarz et al., 2006). This configuration allows integrating the platforms of the station into the tunnel limiting the excavation of complicated caverns or enclosures between diaphragm walls where unfavourable soils, groundwater conditions and limited available space are found.

87% of the tunnels length was excavated by tunnel boring machines and the rest using diaphragm walls (12%) or by mining (1%). Five tunnel boring machines were used simultaneously: two EPB machines 12.06 m in diameter, one dual-mode TBM 11.95 m in diameter, and two EPB machines 9.4 m in diameter. The two machines of least diameter were used to excavate the section of the L9 running through the Llobregat delta, where the stations are built the shallowest between diaphragm walls using the cut-and-cover method and where the two trains run in parallel.

Both lines include a total of 52 stations: 30 are shaft-type stations, 17 are stations excavated between diaphragm walls, and 5 were constructed on surface in viaduct sections. The shafts have diameters of 26 and 33 m, and depths of up to 70 m. They connect the surface with the station hall, and that with the upper and lower platforms inside the tunnel.

3. Geological setting

The geological materials crossed by L9 and L10 lines can be grouped into four main types: recent Quaternary, ancient Quaternary, Neogene and Palaeozoic (Fig. 1).

The recent Quaternary unit forms the Besòs and Llobregat deltas. They are mainly composed of soft sediments of gravel-bearing sand and silt, of grey to yellow colour. Its thickness increases from inland to the coast line, where it reaches up to 50 m. These sediments correspond to the Holocene period (Marqués, 1984; Gàmez et al., 2009; Velasco et al., 2012).

The ancient Quaternary unit forms the Barcelona plain and its extension beneath the younger sediments of the Besòs and Llobregat deltas. This is a very heterogeneous unit mainly composed of reddish clay and silt, with frequent beds of metamorphic gravel and horizons of carbonate nodules of edaphic origin. These are colluvial and alluvial sediments coming from the erosion of the Collserola Palaeozoic chain (Llopis-Lladó, 1942; Solé-Sabarís, 1963). The thickness of this formation is highly variable because it fills a very irregular pre-Quaternary palaeotopography. It ranges from a few metres to more than 30 m. A late Pliocene to Pleistocene age is considered for this unit (Riba and Colombo, 2009).

The Neogene is found beneath the Quaternary deposits of the Barcelona plain and the Besòs and Llobregat deltas. It includes three main sedimentary units: Pliocene, Middle Miocene and Early Miocene. The Pliocene unit is mostly composed of grey marl of deep marine origin. Above this marl, layers of greenish siliceous sand of shallow marine origin are also present in the Barcelona plain area. As a whole, they form a sequence of about 100 m in thickness, which covers an old erosive surface excavated on the top of the Miocene deposits (Vicente, 1986). The Middle Miocene unit forms a sequence of about 200 m in thickness characterized by a cyclic succession of layers of quartz–feldspar sand, quartzose gravel, silt and marl, of alluvial to deltaic origin (Gómez-Gras et al., 2001; Salvany, 2013). The sand and gravel layers have been hardly lithified in part by siliceous cement becoming layers of sandstone and conglomerate (Parcerisa et al., 2001). These rocks are mainly located in the Montjuïc Mountain, while in the neighbouring planes of Barcelona and the deltas they are dominated by unconsolidated sediments with minor cemented layers. The Early Miocene unit forms a monotonous sequence of gravel-bearing clay of reddish colour up to 100 m in thickness, of alluvial origin, which covers the Palaeozoic rocks.

The Palaeozoic unit forms the Collserola chain and its extension beneath the Barcelona plain. It includes a wide variety of metamorphic rocks (hornfels, slates, schists, quartzites), as well as sedimentary (limestones, sandstones, conglomerates) and granitic rocks, ranging from Ordovician to Carboniferous age (Julivert and Duran, 1990). These rocks have been strongly folded and broken by Variscan and Alpine tectonics (Santanach et al., 2011). The Miocene deposits have minor tilting and faulting structures caused by the post-Alpine extensional tectonics that affected the western Mediterranean region during the Neogene period. The Pliocene and Quaternary units are generally undeformed deposits.

In the study area, the geological information provided by the exploratory boreholes of L10 and L2 (still not constructed) lines is available (Figs. 2 and 3). The two lines allow two complementary cross-sections perpendicular to each other, which cut the recent and ancient Quaternary and Miocene units of the northern margin of the Llobregat delta, close to the Montjuïc Mountain.

The recent Quaternary unit forms a wedge-shaped sedimentary unit that thickens towards the coast. It consists of six main sedimentary layers: H1 represents a coarse-grained alluvial sediment directly deposited on the pre-Holocene deposits. It corresponds to the layer of boulders that caused the jamming of the tunnelling machine. H2 is a layer consisting in coarse sand with small gravels representing beach sediment. H3 is a layer composed of silt of dark grey colour and distal prodeltaic origin. H4 is a layer formed of silty fine sand of grey colour and proximal prodeltaic origin. H5 is a layer composed of coarse sand with gravel beds and delta front origin. On the top, H6 is a layer consisting of brown silt of delta plain origin. The uppermost part of this H6 layer forms an anthropic fill of up to several metres thick (layer A) resulting from the construction works of the city.

For an engineering purpose, the stratigraphy of this Holocene delta was simplified in three main layers: a basal layer of boulders (H1), a middle layer of sand (H2 to H5), and an upper layer of silt (H6). Their main geotechnical characteristics are summarized in Table 1.

Along the L10 cross-section (Fig. 2), the layer of boulders exhibits a thickness between 1.5 and 6.8 m and is gently inclined towards the SE. Its base is located 3.5 m below sea level in the northern part of the section, while it is recorded 30 m below the sea level by the southern boreholes that reach to cut it. This is a well-graded layer with gravel and boulders of rounded shapes that range from a few centimetres to more than 1 m (Figs. 4 and 5). The grains are mainly sandstone and conglomerate fragments coming from the Montjuïc Mountain. The main thickness of this layer is located close to the Foc-Cisell station. In boreholes around this station (for instance SZF-13, SZF-14, L2-40 or L2-38), the lower part of this layer is mainly composed of gravel of grain-sizes inferior to 10 cm, while the boulders concentrate in its upper part. Towards the SE, the layer becomes thinner (between 1.5 and

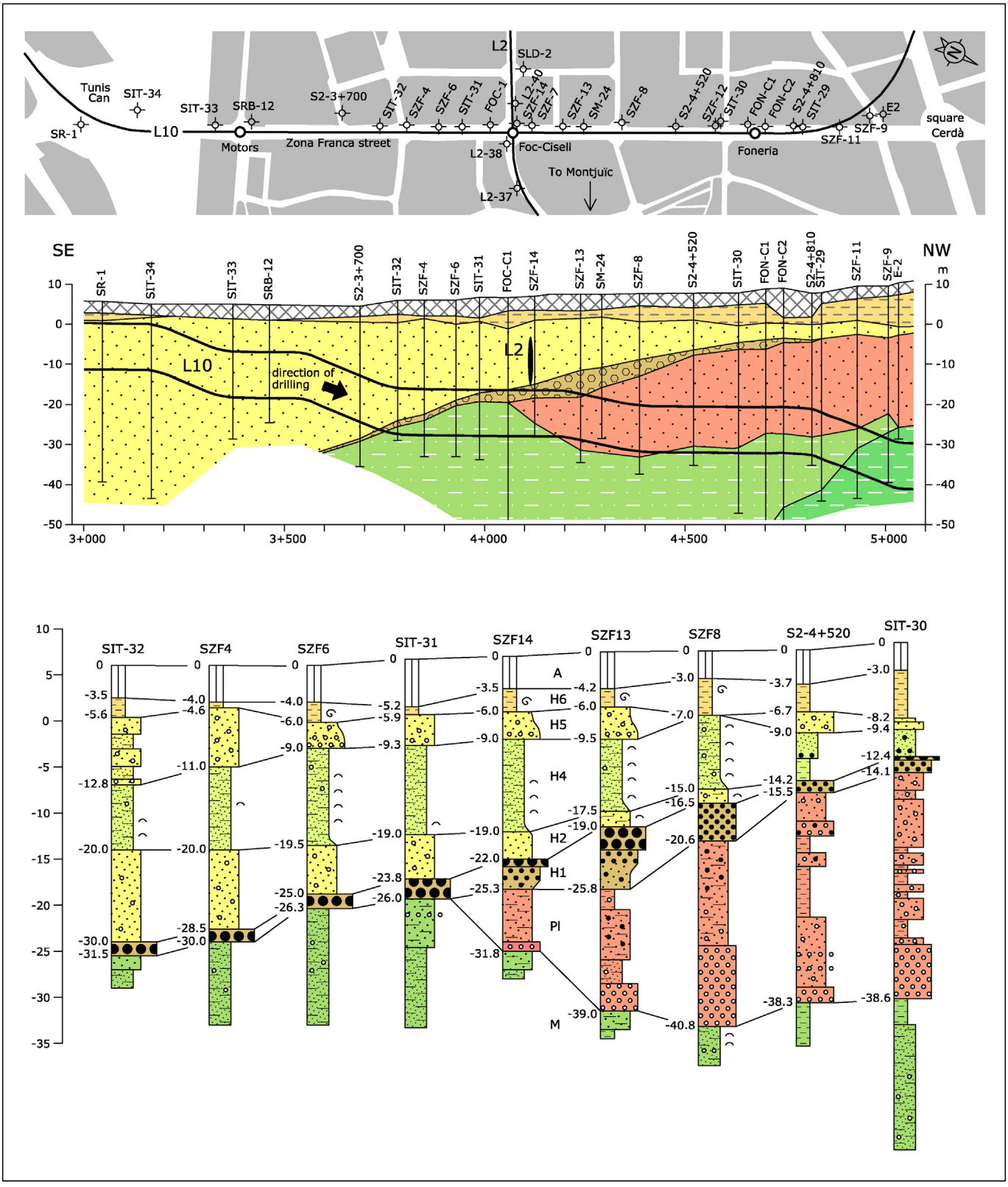

Fig. 2. Geological cross-section and representative boreholes of the L10 line into the study area.

2.5 m in thickness) and is only composed of boulders directly covering the Miocene basement. Towards the NW, the layer also becomes thinner and the boulders are scarce although always located in its upper part.

In L2 cross-section (Fig. 3), the layer of boulders has a more regular thickness of about 4 m and shows a gentle inclination towards the SW. Delta inwards, shortly after the Foc-Cisell station the boulders of this layer quickly disappear and the layer becomes only composed of gravel

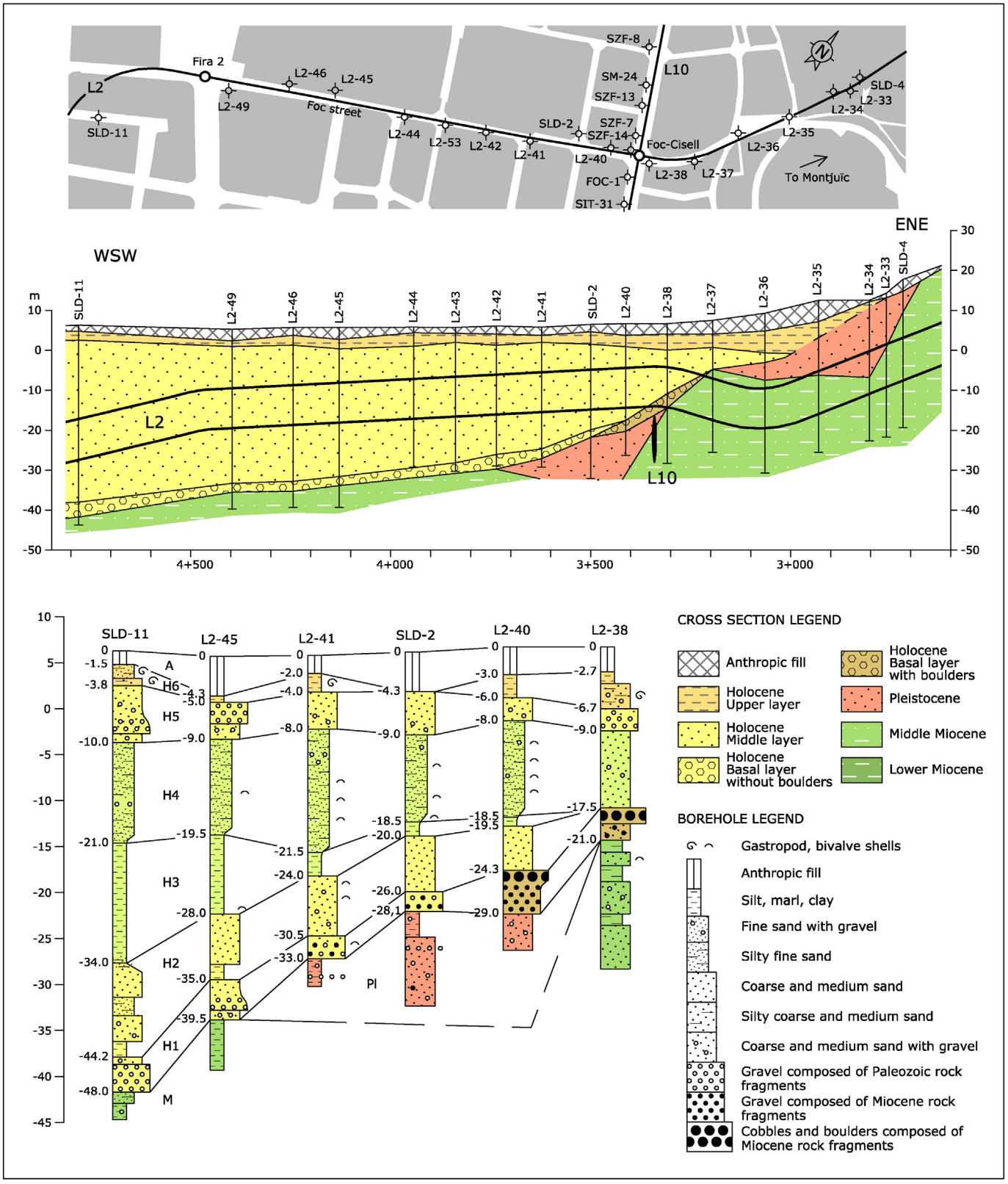

Fig. 3. Geological cross-section and representative boreholes of the L2 line into the study area.

rarely exceeding 10 cm in grain size, mixed with abundant coarse sand. In the same direction, the gravel composition grade from Miocene rock fragments to dominant metamorphic rock fragments coming from the Collserola chain.

The geology of the Llobregat delta has been studied in detail by Gàmez (2007) from cores of hydrogeological and geotechnical boreholes. According to this study, the Llobregat delta is the sum of four superposed deltas developed through Quaternary glaciation-related

Table 1
Geotechnical characteristics of the materials crossed by the tunnel boring machine in the study area (after GISA, 2002).

	Apparent density	Saturated density	Submerged density	Uniaxial compression	Cohesion	Friction angle	Poisson's ratio	Young's modulus
	γ_n	γ_{sat}	γ'	qu	C′	ϕ′	ν	E
	kN/m^3	kN/m^3	kN/m^3	MPa	t/m^2	°		MPa
Anthropic fill	18	19	9	–	3	30	0.35	10
Upper layer of silt	17.2	20.1	10.1	0.647	2.5	29	0.35	15
Middle layer of sand	17.8	20.2	10	0.11	1	34	0.33	15
Basal layer of boulders	18	22	12	91.88[a]	1	45	0.3	20
Miocene basement, sand	18.4	21.2	11.2	0.158	1	33	0.33	60

[a] Calculated for a single boulder.

eustatic cycles. The uppermost delta corresponds to the Holocene period, while others correspond to the Pleistocene. The above-referred ancient and recent Quaternary units of the study area correspond respectively to the third (late Pleistocene) and fourth (Holocene) deltas described in Gàmez (2007). The two lowest deltas are inexistent in this area.

Each delta forms a sedimentary sequence that expands from onshore to offshore, bounded by a main basal erosive surface (Gàmez et al., 2009). This erosive surface removes the uppermost sediments of the underlying deposits. It represents a low standing of the sea level related to a glacial maximum period. During the subsequent sea deglaciation-induced level rise, the erosive surface gradually became

Fig. 4. Excavation of the shaft-station of Foc-Cisell. (A) General view of the removed layer of boulders in the shaft; (B) detail of some boulders showing its characteristic well rounded shapes; (C) detail of a single boulder showing small borings (arrows) made by lithofagous fauna.

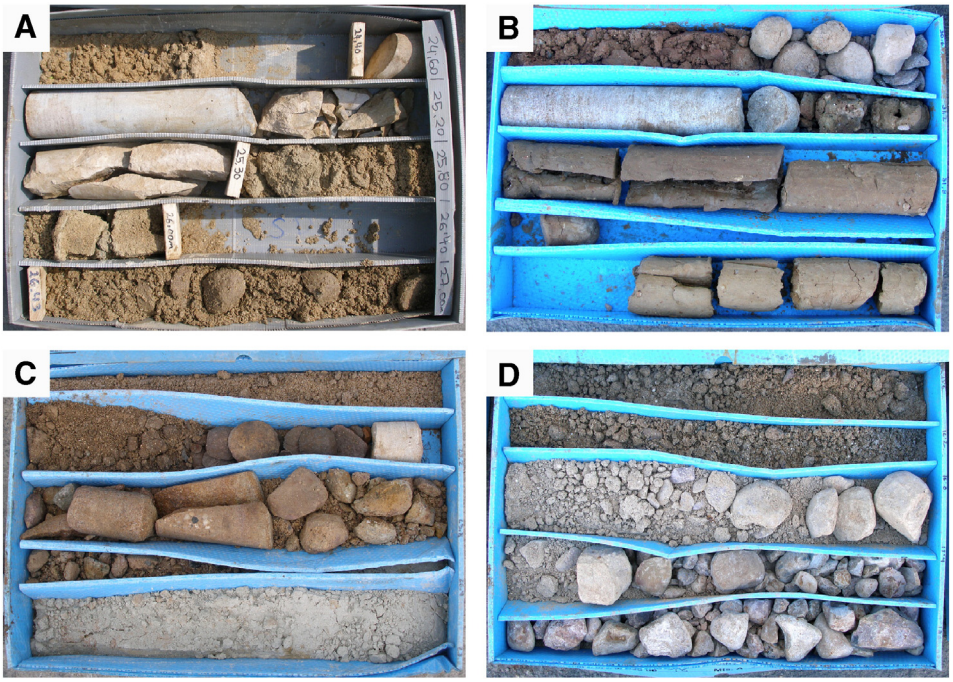

Fig. 5. Cores of the layer of boulders: The top and bottom are respectively in the upper-left and lower-right parts of each box, and have a length of 3 m. (A) Borehole L2-40 between 24 and 27 m of depth. Between 24.3 and 25.3 there are fragments (broken by the drilling machine) of a single boulder of sandstone. Above it there is coarse sand from the H2 layer. Below there are the gravel and coarse sand of the lower part of the layer of boulders. (B) Borehole SZF-7 between 30 and 33 m of depth. Between 30.4 and 31 m there are fragments of a single boulder of sandstone. Above it there are coarse sand and small gravels from the H2 layer. Below there is brown clay of the ancient Quaternary. (C) Borehole SZF-6 between 24 and 27 m of depth. Between 25 and 30 m there are fragments of boulders and subrounded gravel. Above it there is the sand from the H2 layer. Below there is white fine sand from the Miocene basement. (D) Borehole SZF-8 between 15 and 18 m of depth. The upper half of the core consists of sand with small gravels from the H2 layer. The lower half is subrounded gravel from the layer of boulders. In this borehole, there are not any boulders. (For interpretation of the references to colour in this figure legend, the reader is referred to the web version of this article.)

buried by new sediments, thus creating a new deltaic sequence. Therefore, only the lower parts of the Pleistocene deltaic sequences are preserved while the Holocene delta is complete as it has not been affected by any new sea level fall yet. Its layers form a complete depositional sequence of the delta with a basal erosive surface (low stand), a lower part (H1 and H2) of retrogradant alluvial to beach sediment (transgressive stand), and an upper part (H3 to H6) of progradant deltaic sediment (high stand). This Holocene delta started to develop after the last fall of the Mediterranean sea level about 20,000 years ago (Last Glacial Maximum), and continued to grow until recent historical time (Marqués, 1984).

The main thickness of the layer of boulders in the L10 cross-section coincides with the outlet of an ancient ravine inserted in the SW slope of the Montjuïc Mountain (Fig. 6). This ravine and its tributaries form a drainage basin that covers the main part of the southern half of this mountain. At present, this drainage basin is difficult to identify because it has been intensively modified by the mining (open pits) and urban constructions of the mountain, mainly developed during the last century. However, it remains well-defined in the ancient topographic map by Cerdà (1859), which was drawn before the major transformation of the mountain (Fig. 6).

The location, structure, grain size and grain composition allow interpreting the layer of boulders as the sediment of a small alluvial fan settled in the outlet of the above-referred ravine (Fig. 6). The alluvial fan would have its origin in the speeding up of the Montjuïc denudation due to the increased topographic gradient that resulted from the last sea level fall. This fall was of about 120 m below the current sea level (Antonioli, 2012), thus nearly doubling the current height of the mountain, going from 175 m at present to about 300 m at that time. The Foc-Cisell area would be the apex of this alluvial fan, thus accumulating the alluvial sediment of biggest grain size (boulders and biggest gravels). Gravels of gradually minor size deposited inward the delta. In the same direction the alluvial fan connected with coeval alluvial sediments of Palaeozoic composition nourished from the Collserola source area. The boundary between the two alluvial systems is difficult to draw due to the paucity of available subsoil data and the gradual transition between them.

The L10 cross-section shows a marked asymmetry in the boulders arrangement. The boulders are mainly concentrated in the southern half of the alluvial fan and are scarce or non-existent to the North. This feature can be explained by the inclination to the SE of the erosive surface that supported the fan, which favoured the deposition of the largest alluvial grains in the same direction (Fig. 6). The proximal parts of the fan would also have accumulated blocks fallen from the SW slope of the mountain, thus explaining the presence of boulders in the northern half of the fan.

According to this sedimentary interpretation, the expected shape of the gravel and boulders would be between moderately rounded (short alluvial transport) to angular (fallen rocks). However, as stated above, their shapes are always well-rounded (Fig. 4). Besides, the surface of the boulders shows frequent lithofagous borings and occasionally biofoulings (Fig. 4C). Such features lead to interpret that a marine reworking of the alluvial sediment occurred. This reworking would be caused by sea wave action during the sea level rise and consequent alluvial fan flooding. Thus, it would have resulted in a recessive boulder beach (Fig. 7).

Some current boulder beaches of the world have similar origins (Carter and Orford, 1993; Haslett, 2000). They result from marine reworking of ancient glacial tills or other boulder-bearing sediments (Davidson-Arnott, 2010). The sea waves take away the finer grains (silt, sand and small gravel) and concentrate the biggest thus forming gravel or boulder beaches where the rock grains are characterized by having well-rounded shapes. The abundant sandy matrix found in the basal layer can be understood as sand percolated during sedimentation of the H2 layer above.

The ancient Quaternary unit crossed by L10 line fills a palaeo-channel excavated on Miocene deposits. It reaches a thickness of 23 m below the Foneria station. Gravels rarely exceed a grain size of 10 cm and are

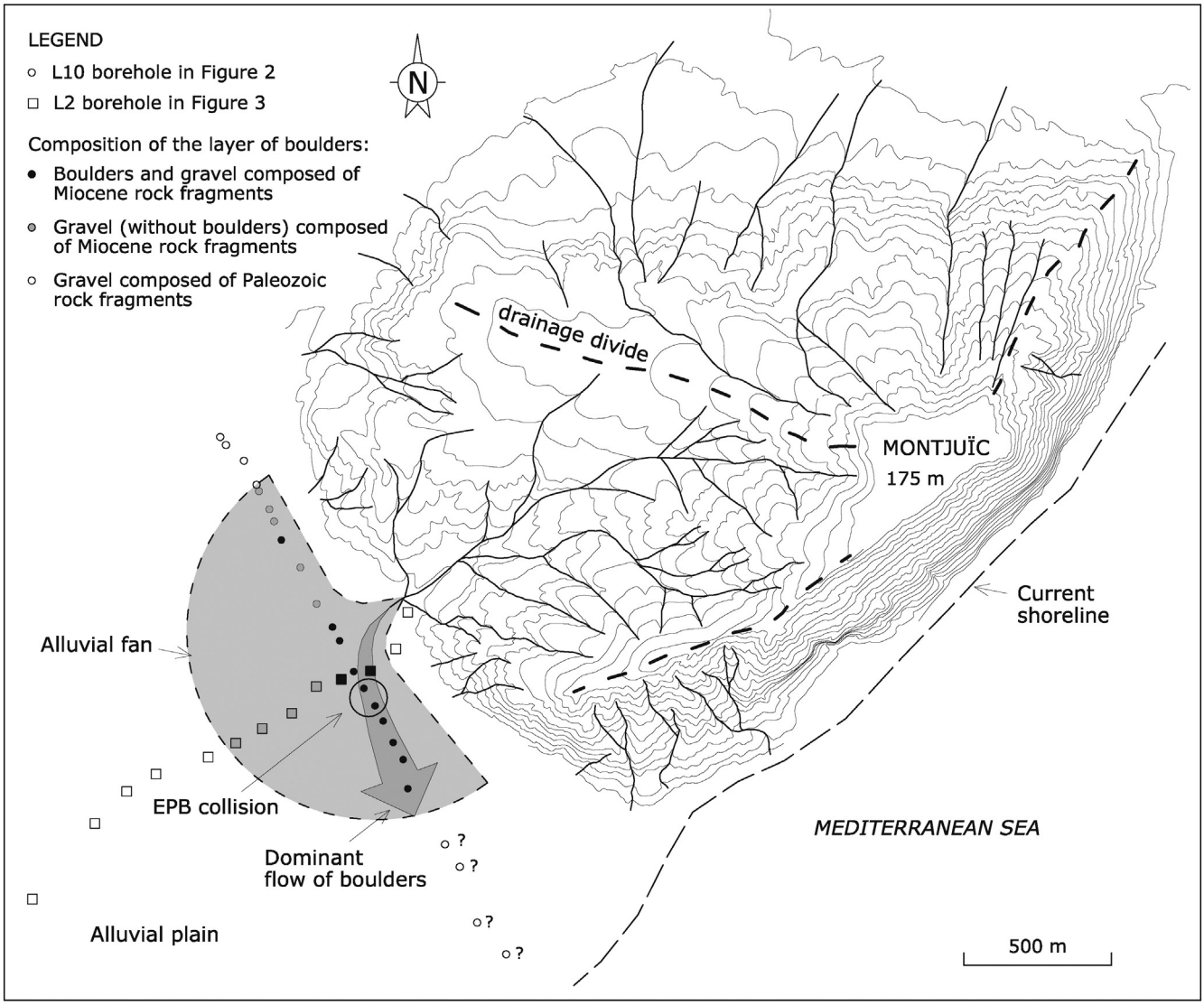

Fig. 6. Map of the Montjuïc Mountain and the interpreted alluvial fan that formed the layer of boulders. The topography of Montjuïc Mountain has been adapted from the ancient map of Barcelona drawn by Cerdà (1859).

mostly composed of metamorphic rock fragments from the Collserola chain. Subordinate sandstone and conglomerate rock fragments coming from the Montjuïc Mountain are also found. Therefore, for this sequence, the Montjuïc Mountain was also a source area, and a similar lag deposit of boulders would be expected. However, boulders are lacking, which has not a clear explanation.

4. Problems and solutions during the excavation of the L10 tunnel

The L10 line through the Llobregat delta was excavated with an EPB S-221 tunnel boring machine of 12.06 m of diameter with a cutterhead designed to dig soft and mixed grounds. It was manufactured in Germany by Herrenknecht (Table 2). The excavation began in January 2009 near the Barcelona harbour. The EPB machine started in the launch shaft of Can Tunis at kilometric point 3 + 100 (henceforth k.p.), digging the sand of the middle layer of the delta. On March 25, after about three months of excavation, at k.p. 3 + 716 begun the first excavation difficulties with changes in the behaviour of the tunnelling machine parameters. On that day some boulders appeared in the conveyor belt pointing out the first contact of the tunnel boring machine with the layer of boulders (Fig. 8A). Despite this situation, the excavation continued. On March 28, at k.p. 3 + 785 a significant decrease of the machine performance was recorded. At this point a high elevation of the thrust force, cutting wheel displacement and torque parameters occurred, together with a significant decrease of the machine penetration (Fig. 9). Additionally to this low performance, a high fluctuation of the earth pressure began in the tunnel face because of the difficulty of keeping the gate of the screw conveyor closed due to the boulders jam. This jamming was first observed at k.p. 3 + 774. On March 29 the tunnelling machine reached k.p. 3 + 789 with increasing difficulties. At this point the EPB was stopped to check its cutter tools.

Traditionally, the maintenance operations of EPB cutterheads to repair and replace the cutter tools are performed by means of hyperbaric interventions (Lang, 2014). However, in this case the hyperbaric intervention was not easy because the sandy and gravel nature of the excavation face caused repeated pressure losses during the creation of the air bubble. On March 29, several failed attempts of hyperbaric interventions were made. In order to try new hyperbarics, on April 2 the machine was moved forward up to k.p. 3 + 793. During this new advance the problems increased due to the fluidity of the materials acquired from the bentonite additives used during the first hyperbaric interventions. In order to find a stable face, on April 3 the machine moved again to k.p. 3 + 797. On that day the conveyor belt took out disc fragments of the cutterhead and bentonite and foam leakages were

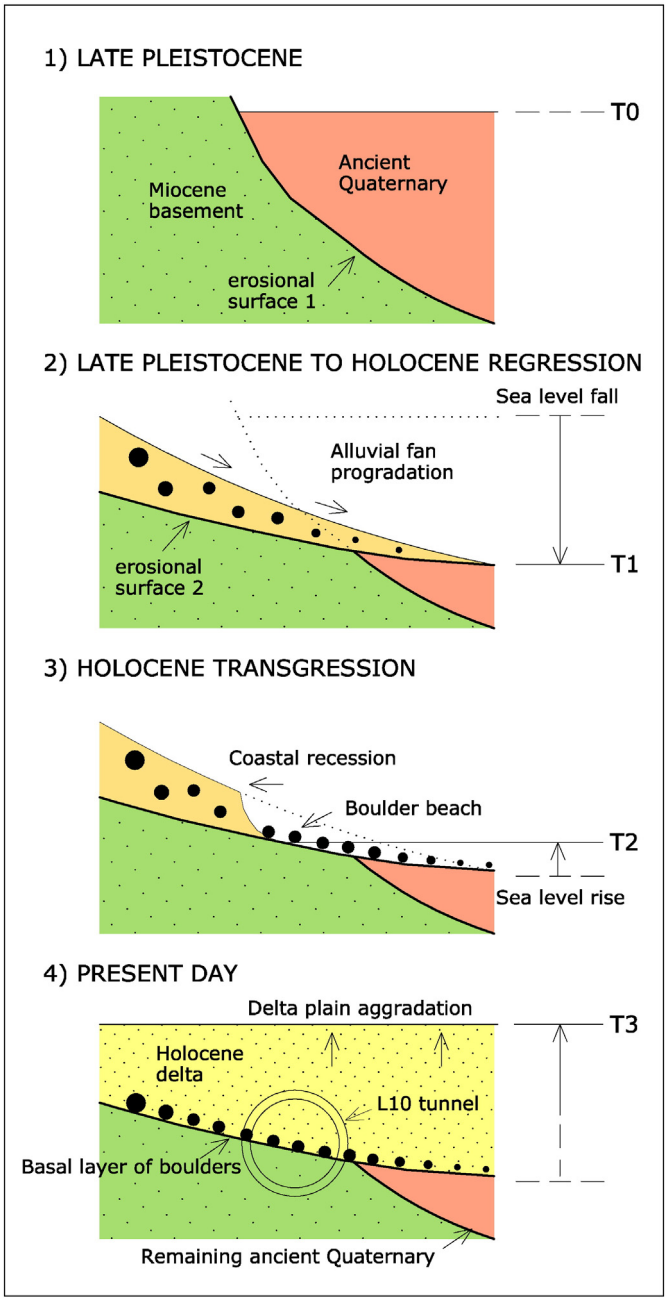

Fig. 7. Schematic cross-sections from Montjuïc Mountain (left) to Llobregat delta (right) summarizing the main sedimentary events interpreted for the layer of boulders intersected by L10 line.

detected towards a big waste water collector of 12 m^2 of section located above the tunnel. Moreover, a strong smell coming from this collector reached the tunnel. Those aspects point out that a physical connection between the tunnelling machine and the collector occurred. All these reasons led to the final stoppage of the tunnelling machine (Fig. 8B).

Another cause of problems was the anomalous settlements triggered since the first excavation difficulties on March 25 (Fig. 10). According to the auscultation readings, the settlements were mainly originated by the high fluctuations of pressure in the tunnel face resulting from the jamming of the boulders in the gate of the screw conveyor. The main settlements occurred during the excavation of the last metres before the stoppage of the tunnelling machine on April 3. Close to this point the settlement reached −80 mm (Fig. 10).

Hyperbaric intervention was finally possible at k.p. 3 + 798 with the aid of foam injections from the surface. The preliminary review

Table 2
Technical characteristics of the tunnel boring machine used for the excavation of the L10 line in the study area.

	EPB S-221
General	
Total length	92 m
Min. radius	300 m
Design radius	250 m
Max. water pressure	4.5 bar
Segment data	ID 10.9 m
	OD 11.7 m
	W 1.8 m
Shield	
Type	EPB
Min. curve radius	250 m
Nominal diameter	12,060 mm
Diameter, middle section	12,045 mm
Diameter, tail shield	12,030 mm
Length	10,995 mm
Tailskin seal system	3 rows of brushes
Mortar injection lines	10
Cutterhead	
Type	closed
Diameter	12,060 mm
Opening ratio	33%
Tools	264 scrapers
	16 buckets
	42 pieces 17″ disc cutters
Cutterhead drive	
Type	Hydraulic
Number of motors	24
Nominal torque	38,022 kNm
Break even torque	45,626 kNm
Variable speed	0–2.6 rpm
Electrical power	4000 kW
Thrust cylinders	
Quantity	38 pieces (2 × 19)
Thrust force	120,759 kN at 350 bar
Exceptional thrust force	138,010 kN at 400 bar
Stroke	2600 mm
Advance speed	0–80 mm/min

of the cutterhead allowed observing significant weathering and breakages of the cutter tools, as well as important damages on the structure, Hardox plate and scraper supports (Fig. 11). The repair required welding tasks under atmospheric pressure conditions in a stable and sealed environment.

At the stoppage point, the excavation face intersected three layers (Fig. 8B): the upper half consisted in the middle sandy layer of the delta; practically in the tunnel axis the basal layer of boulders with a thickness of 1.5 m; and the lower part contained the sand of the Miocene basement. At this point, the tunnelling machine was 22 m below the surface and 13 m below the water table.

The easiest and fastest technical solution to repair the cutterhead would have been the excavation of an enclosure between diaphragm walls at its front. However, the existence of the waste water collector prevented this option and lead to the construction of a solid block by jet grouting and further embedding of the tunnelling machine into the block, and finally the digging of a mine inside the block allowing the workers access to the excavation face to repair the cutterhead (Fig. 8C, D and E).

The built block extended from some metres above the tunnel crown to some metres below the tunnel axis, and had a parallelepiped shape of 9.54 m in length, 18.55 m in width and 20 m in height (Fig. 12). It included a protection boundary of 3 m in its lower part and sides, and 5 m above the tunnel. The block was built from the surface with a

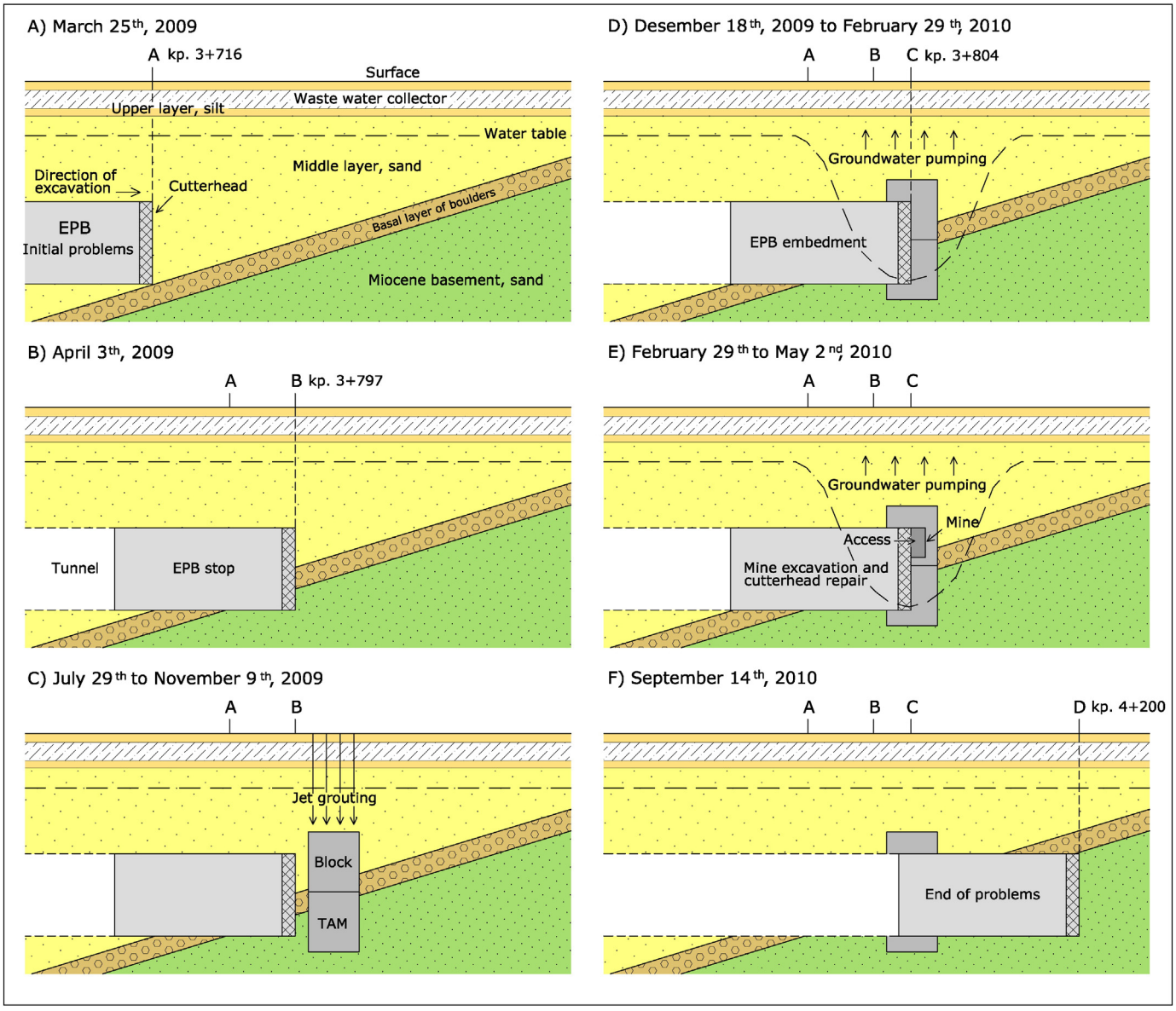

Fig. 8. Summary of the tunnel boring machine evolution from the first problems with the layer of boulders until they were solved.

triangular network of jet grouting columns (Fig. 13). The columns of the inner part of the block were performed with a separation of 1.3 m from its centre. For each column a theoretical diameter of 1.65 m was assumed, thus allowing an overlap between columns of 0.35 m. The peripheral columns of the block were arranged in a narrower manner, with a separation of 1.15 m. In addition, a line of 18 micro-columns of jets of lesser pressure and 1 m in diameter, separated 0.8 m and with an overlap of 20 cm, was also built in front of the cutterhead. This line was devised to create a safety barrier to prevent potential damages to the machine during the building of the block. As a whole, a total of 137 columns were performed, which represents the drilling of 5242 linear metres and the grouting of 2718 linear metres using the superjet-grouting technique (Zuloaga, 2004).

After building the block, the geotechnical survey designed to verify its uniformity detected sealing deficiencies in the layer of boulders and the Miocene basement, due to deficiencies in the treatment of these layers by jet grouting. To reduce its permeability, a reinforcement treatment using new injections from the surface was performed. This reinforcement was made with Tube-à-Manchette (TAM) injections (Warner, 2004), which consisted in PVC pipes with 0.5 m-long rubber sleeves in the deepest fifteen metres and blinds in the rest, which allowed successive injection passes. The annular space between the pipes and the ground was sealed with a mortar grout prepared with one part of water to one and a half of cement and mixed with 2% of bentonite. The TAMs reached depths of 2 m below the tunnel section, namely 36 m from the surface.

The TAM injections started first in the layer of boulders and continued later in the Miocene sand. The layer of boulders was treated with concrete grout and micro concrete grout of progressively finer size (A32, A12 and A6 types). The criteria for ceasing injections were pressure (maximum 5 or 8 bars, depending on the number of passes) or volume (1000 l of concrete, 500 l of micro concrete). The silty sand of the Miocene basement was treated only with silica gels, following similar ceasing criteria (5 or 8 bars of pressure, 300 l of volume).

The reinforcement work by TAM injections lasted a month. In sum, 73 TAM injections were performed, which represent the drilling of 2628 linear metres and the injection of 1018 linear metres through 1940 rubber sleeves. They consumed a total of 53,000 l of concrete grout, 1650 l of micro-concrete grout A36, 1500 l of micro-concrete grout A12, 10,200 l of micro-concrete A6, and 13,800 l of silica gel grout.

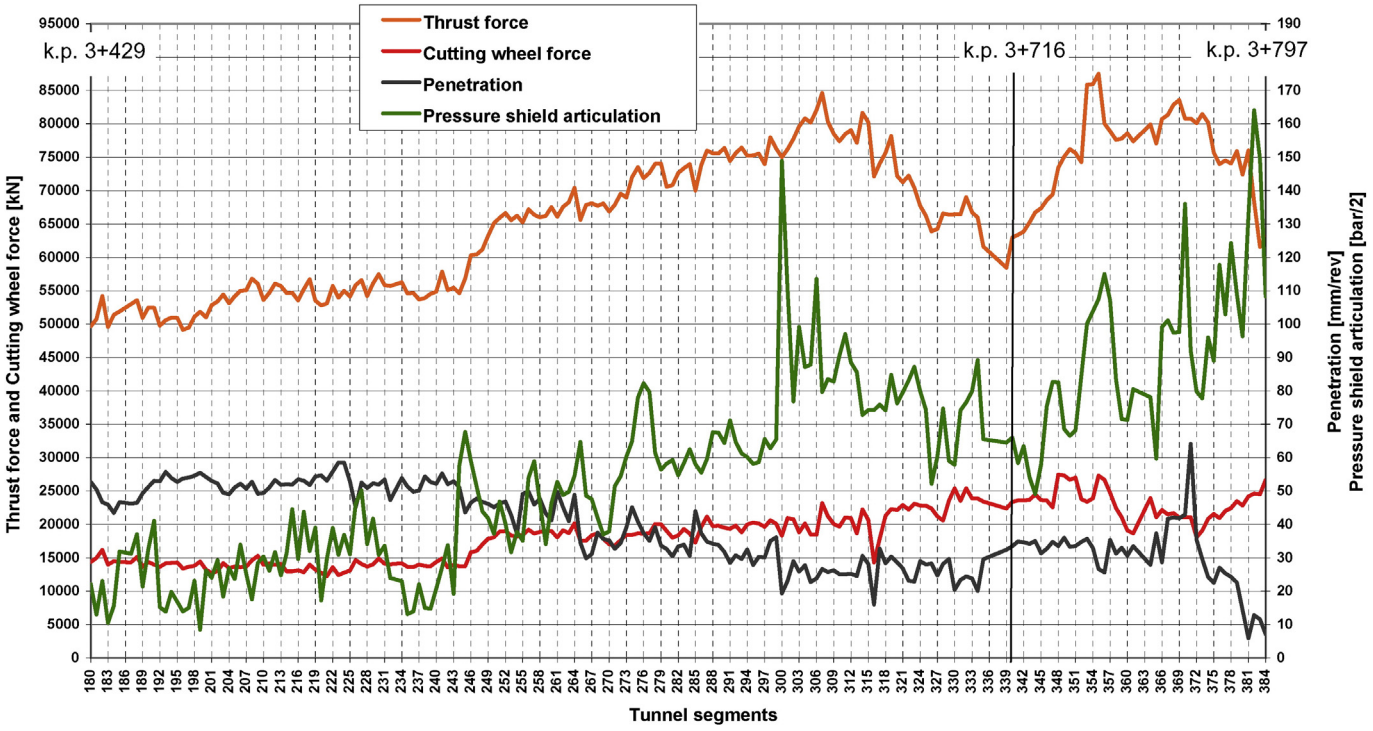

Fig. 9. Evolution of some excavation parameters of the tunnel boring machine between k.p. 3 + 429 (segment 180) and the stoppage point at k.p. 3 + 797 (segment 385). The first contact with the layer of boulders and the beginning the first excavation difficulties occurred at k.p. 3 + 716 (segment 340). Segment 372 corresponds to k.p. 3 + 772 when the jamming of boulders in the screw conveyor begins. Segment 378 corresponds to k.p. 3 + 785 when the performance of the tunnelling machine begins to decrease significantly. Each tunnel segment has a length of 1.8 m.

The completion of the block and its reinforcements was followed by the injection of a bicomponent expanding foam from the surface to fill the possible remaining holes in the ground caused by the removal, after various attempts, of the hyperbaric interventions. Then, the tunnelling machine was restarted and embedded into the block. Once newly stopped at k.p. 3 + 804, the annular space between the EPB

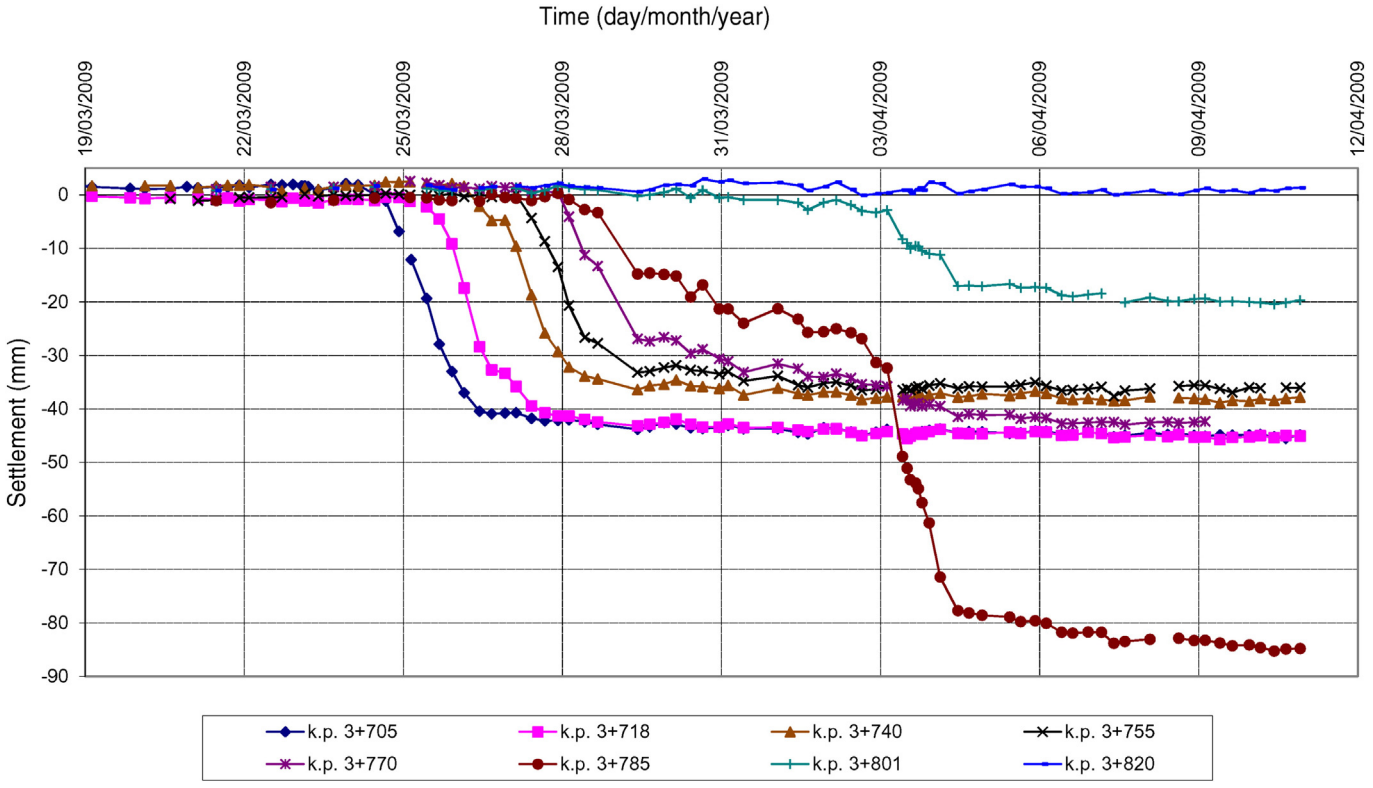

Fig. 10. Settlements recorded by several monitoring points along the tunnel, during the collision of the tunnel boring machine with the layer of boulders. Profile between kilometric points 3 + 700 and 3 + 831.

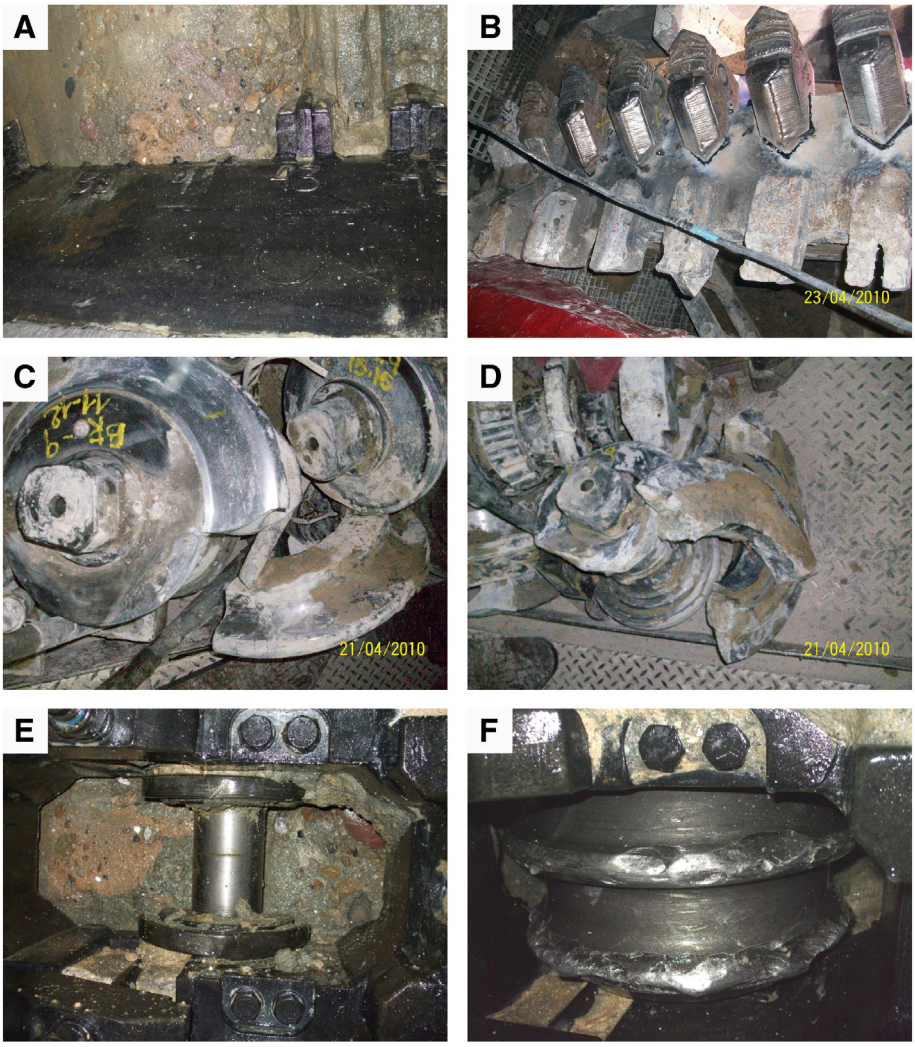

Fig. 11. Damages of the cutterhead tools. (A) Scraper supports missing, (B) scrapers strongly worn (bellow) and new line of scrapers to substitute the ones damaged (above), (C and D) disc cutters broken, (E) remaining support after the disappearance of a disc cutter, (F) disc cutter badly worn.

shield and the ground was closed with expanding foam (Geofoam) to ensure sealing behind the block.

Before excavating the mine, several permeability tests in the block and surrounding ground were made. Results made it necessary to depress the water table to enable the reparation works at atmospheric pressure. This was a necessary condition to ensure the access into the block and safety of the repairing workers. To depress the water table, a total of 21 pumping wells were drilled with lengths between 21 and 37 m, 8 inside the block and 13 in the external unaltered materials (Fig. 14). The wells were drilled with diameters of 273, 300 and 550 mm (the largest sections outside the block), and were coated with PVC tubes of 200, 180 and 400 mm respectively. They were equipped with pumps with a power between 5.5 and 30 kW. All the pumps reached regular extractive volumes of water of some 650 m^3/h. To evacuate this large volume of water, a complex water drainage network supported by a powerful electric system had to be performed.

To monitor the water table during pumping, a total of 10 piezometers were installed inside and outside the block. These piezometers incorporate 27 pressure sensors monitoring the water table of the three geological layers and water volume counters to measure the amount of water extracted from each well.

In addition, an auscultation system was performed to monitor the possible movements caused by water extractions. The measuring instruments of this system were installed in the ground, in the neighbouring buildings and in the waste water collector. A 24-hour monitoring protocol was drafted to follow any incidence related to pumping actions or ground movements. The pumping of the 21 wells to depress the water table lasted about five months. The water extractions started before the excavation of the mine and extended until the end of the cutterhead repairs. During this time, a total of 1,400,000 m^3 of water was pumped.

Groundwater pumping was the cause of new ground settlements (Fig. 15). In this case there were small settlements of the order of 5 to 15 mm which in part were recovered after the pumping ended and the water table subsequently rose. The sum of these settlements with those initially occurred during the tunnelling machine collision reached values of up to −120 mm.

As soon as the water pressure conditions inside the block were adequate, the excavation chamber behind the cutterhead was gradually emptied and its pressure lowered. Once the required atmospheric conditions were obtained and the risks of instability of the excavation face reduced, the excavation works began. The narrow mine was excavated in two phases (Fig. 16): The first phase (I, in Fig. 16B) allowed repairing the external zone of the cutterhead and the second (II, in Fig. 16B) its central zone.

The repair works lasted for 2 months and mainly consisted in filling the weathered zones by welding of steel plates and recharge cords; welding of anti-wear Hardox plates; welding of ripper supports; welding perimetral disc protection, and substitution of all rippers, blades and rakes, as well as testing, cleaning and repairing the foam

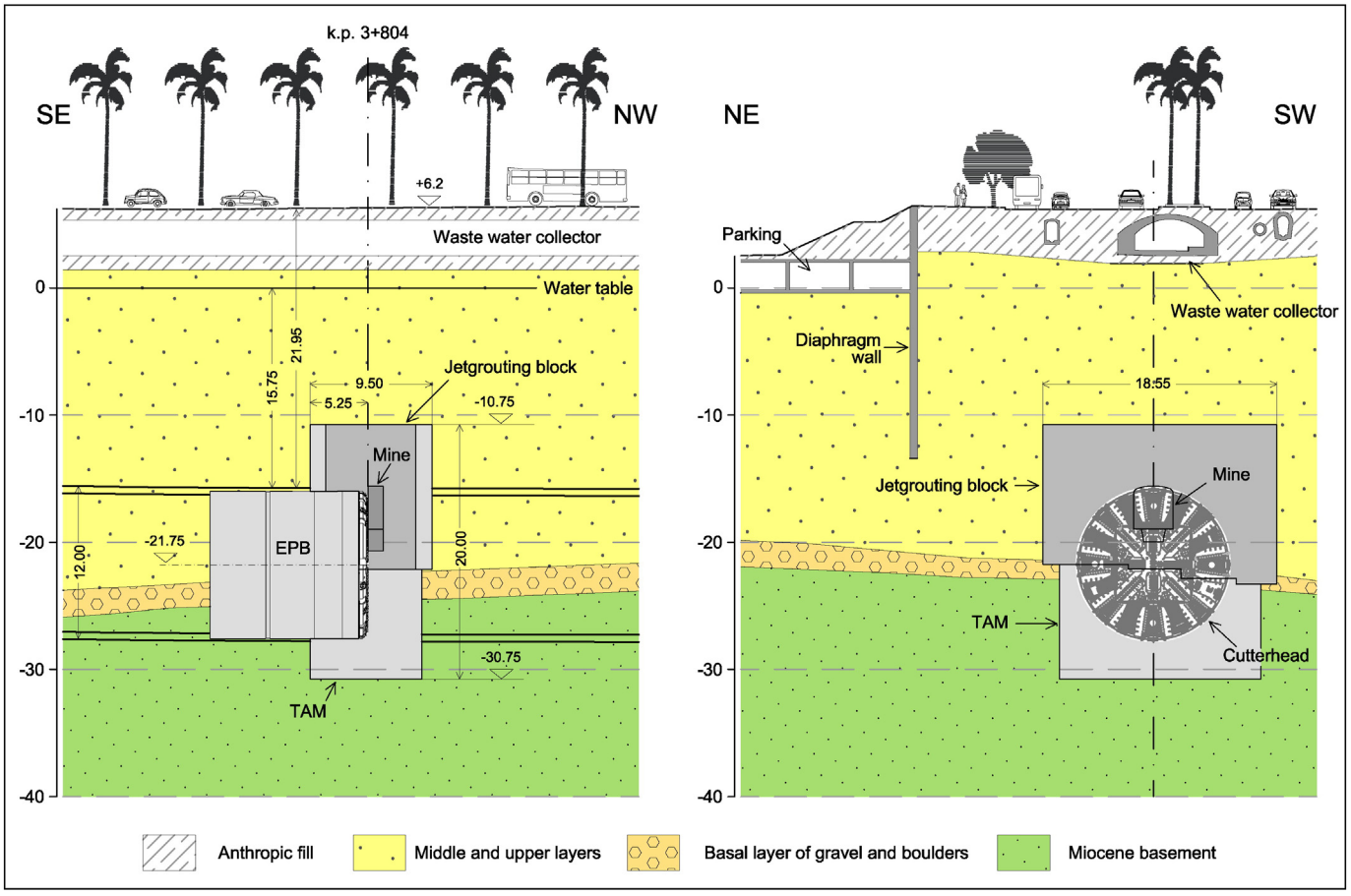

Fig. 12. Longitudinal and transversal views of the jet grouting block and the embedded tunnel boring machine (stage E in Fig. 9).

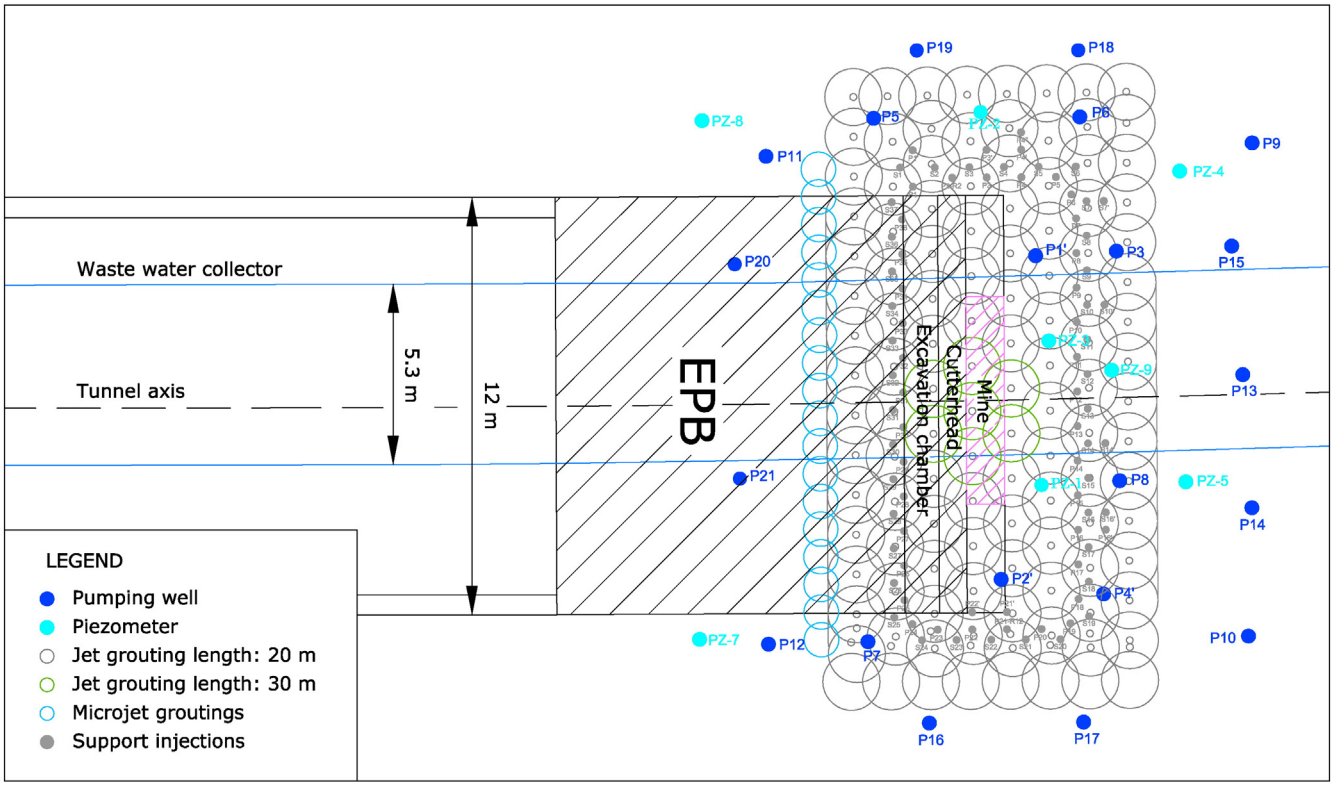

Fig. 13. Plan view of the jet grouting block and the network of pumping wells and piezometers (stage E in Fig. 9).

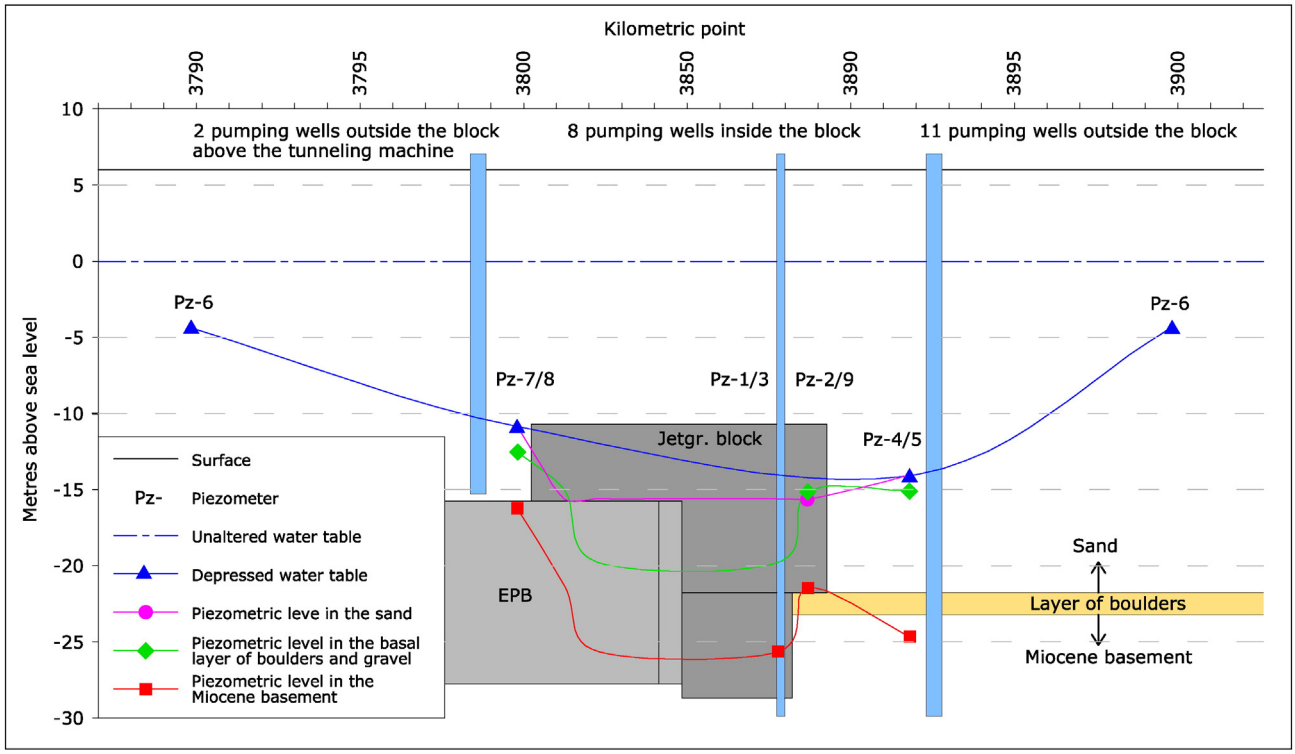

Fig. 14. Piezometric profiles across the jet grouting block during the phase of groundwater pumping (stage E in Fig. 9).

and water lances, and the installation of new high-pressure devices. The stoppage was also used to make improvements in the cutterhead to better excavate the remaining section of the tunnel that would still intersect the basal layer of boulders. These improvements included the installation of a metal detector in the conveyor belt, with acoustic and bright alarms that would turn on in case potential tool fragments from the cutterhead were detected; a powerful electromagnet in the heath output of the belt to catch any metal fragment, and the change of the width of the cutting discs from 1 in. to 1.5 in. to better break further boulders and gravels.

Once the cutterhead was successfully repaired, the tunnelling machine resumed the excavation. Three hundred metres later (at k.p. 4 + 100) the machine reached the shaft of the Foc-Cisell station. At this point, there was a new stoppage to monitor and make additional repairs of the cutting tools. During the next 100 m, the tunnel even crossed the layer of boulders although at progressively greater height.

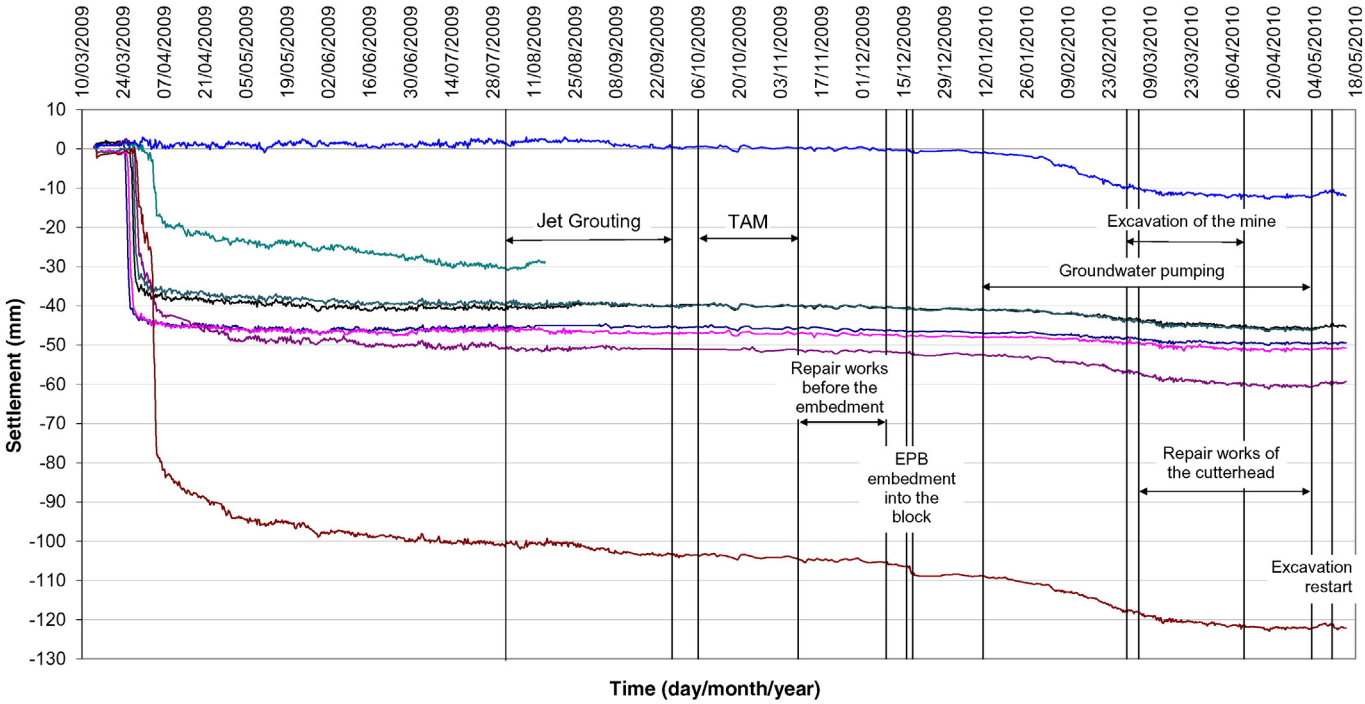

Fig. 15. Settlement evolution since the collision of the tunnel boring machine until the final resolution of problems. Longitudinal profile between kilometric points 3 + 705 and 3 + 820.

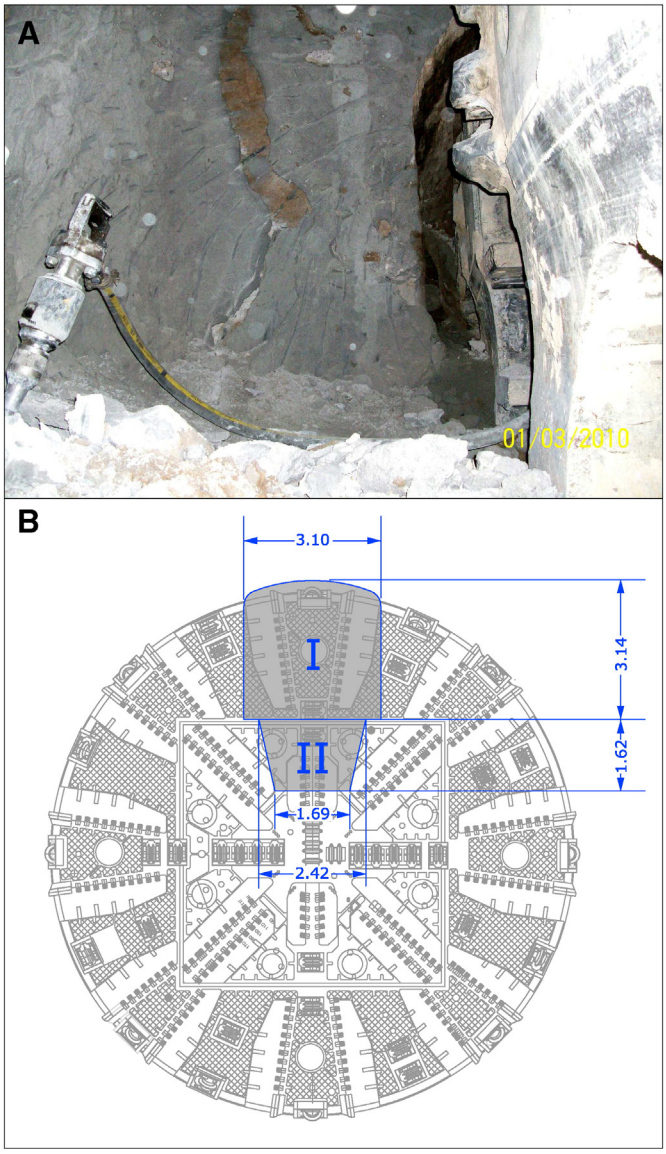

Fig. 16. (A) View of the mine and the cutterhead to their right. (B) Frontal shape and size of the mine and its location with respect to the cutterhead. I is the first chamber excavated to repair the external part of the cutterhead, and II is the smaller lower chamber excavated later on to repair its inner part. The access to the mine was through the elongated-radial slits of the cutterhead (white areas in the drawing).

This section of the tunnel was slowly excavated, changing the excavation parameters and monitoring the cutterhead more frequently. Once k.p. 4 + 200 was surpassed (Fig. 8F), the basal layer of boulders was finally out of the tunnel trace and the tunnelling machine was totally released and could proceed without further problems.

5. Conclusions

Commonly EPB-type tunnel boring machines are good tunnelling devices under uniform soft grounds. The presence of lithological heterogeneities in these grounds need to be considered as potential tunnelling problems and must be carefully analysed.

The study supports the conclusion that the geological conceptual model can be a good tool to better know a given lithological heterogeneity. It allows pinpointing its geometry, structure and extension, as well as its relationships with the surrounding materials. Unknowingly the trace of L10 line along the northern part of the delta coincided precisely with the area of main concentration of boulders of the basal layer: the apex of the former alluvial fan. Should the present geological conceptual model been available at the time, it would have helped in choosing a more adequate path for the tunnel. Thus, a parallel trace some tens of metres into the delta or above the current L10 line tunnel (for instance, the height planned for L2 line in the junction point between both lines) would have avoided this area of main concentration of boulders and thus minimize the problems that occurred.

Under the geological and urban circumstances given, it can also be concluded that the construction of the jet grouting block and its reinforcements, the lowering by pumping of the water table and the subsequent mine excavation to repair and restart the cutterhead were the correct decisions. Previous similar cases were not found to provide a procedure to follow so as to solve the problems, which forced the improvisation of the new engineering methodology presented here. Therefore, this case brings new experience in the field of mechanized tunnelling and becomes potentially useful for future similar situations.

Acknowledgements

The authors would like to thank GISA (Gestió d'Infraestructures SA), as part of the Catalonian Government, and the engineering companies that built L9 and L10 lines (UTE Gorg L9) for their help in providing all the technical documents and data used for this study. The authors would also like to thank the Editor C. Carranza-Torres of the University of Minnesota Duluth, and four anonymous reviewers for their helpful comments to improve the manuscript.

References

Antonioli, F., 2012. Sea level change in western-central Mediterranean since 300 kyr: comparing global sea level curves with observed data. Alp. Mediterr. Quat. 25 (1), 15–23.
Babendererde, L., 2003. Problems of TBMs in water bearing ground. In: Kolymbas (Ed.), Rational Tunnelling. Advances in Geotechnical Engineering and Tunnelling, no. 8, Innsbruck.
Bilgin, N., Algan, M., 2012. The performance of a TBM in a squeezing ground at Uluabat, Turkey. Tunn. Undergr. Space Technol. 32, 58–65.
Bono, R., Ortu, M., Valdemarín, F., 2008. Surface settlement minimization in soft soil when excavating with an Earth Pressure Balance shield. In: Alonso, E., Arroyo, M. (Eds.), Jornadas Técnicas de túneles con EPB. Simulación y Control de la Tuneladora, Barcelona, pp. 129–148.
Cabrera, M.C., Vallejo, A., Valverde, M., Lambán, L.J. (Eds.), 2009. El agua y las infraestructuras en el medio subterráneo. Publicaciones del Instituto Geológico y Minero de España, Madrid.
Carter, W.G., Orford, J.D., 1993. The morphodynamics of coarse clastic beaches and barriers: a short and long-term perspective. J. Coast. Res. 15, 158–179.
Cerdà, I., 1859. Proyecto de Reforma y Ensanche de Barcelona. Ajuntament de Barcelona. Unpublished historical document.
Davidson-Arnott, R., 2010. Introduction to Coastal Processes and Geomorphology. Cambridge University Press, New York.
Day, M.J., 2004. Karstic problems in the construction of Milwaukee's Deep tunnels. Environ. Geol. 45, 859–863.
Deere, D.U., 1981. Adverse geology and tbm tunneling problems. In: Bullock, R.L., Jacoby, H.J. (Eds.), Rapid Excavation and Tunneling Conference Proceedings. University of California, San Francisco (Chapter 13, 13 pp.).
Farrokh, E., Rostami, J., 2009. Effect of adverse geological condition on TBM operation in Ghomroud tunnel conveyance project. Tunn. Undergr. Space Technol. 24, 436–446.
Filbà, M., 2007. Estudio y análisis de la interacción tuneladora TBM-terreno en la excavación de la Línea 9 del Metro de Barcelona tramo 4A (Master Thesis) Universidad Complutense de Madrid.
Filipponi, M., Ganguly, S., 2012. Successful TBM drive in inclined pressure shaft under difficult ground conditions. A Case Study of Hydropower Project Limmern, Switzerland. Proceedings of Indian Geotechnical Conference, Delhi. Paper no. D-401.
Font-Capó, J., Vázquez-Suñé, E., Carrera, J., Martí, D., Carbonell, R., Pérez-Estaun, A., 2011. Groundwater inflow prediction in urban tunneling with a tunnel boring machine (TBM). Eng. Geol. 121, 46–54.
Font-Capó, J., Pujades, E., Vázquez-Suñé, E., Carrera, J., Velasco, V., Monfort, D., 2015. Assessment of the barrier effect caused by underground constructions on porous aquifers with low hydraulic gradient: a case study of the metro construction in Barcelona, Spain. Eng. Geol. 196, 238–250.
Gàmez, D., 2007. Sequence Stratigraphy as a Tool for Water Resources Management in Alluvial Coastal Aquifers: Application to the Llobregat Delta (Barcelona, Spain) (Ph.D. Thesis) Universitat Politècnica de Catalunya, Barcelona.
Gàmez, D., Simó, J.A., Lobo, F.J., Barnolas, A., Carrera, J., Vázquez-Suñé, E., 2009. Onshore-offshore correlation of the Llobregat deltaic system, Spain: development of deltaic geometries under different relative sea-level and growth fault influences. Sediment. Geol. 217, 65–84.

GISA, 2002. Línia 9 del Metro de Barcelona. Projecte constructiu. Departament de Política Territorial i Obres Públiques de la Generalitat de Catalunya. Barcelona. Unpublished raport

Gómez-Gras, D., Parcerisas, D., Calvet, F., Porta, J., Solé de Porta, N., Civis, J., 2001. Stratigraphy and petrology of the Miocene Montjuïc delta (Barcelona, Spain). Acta Geol. Hisp. 36 (1–2), 115–136.

Grandori, R., Jeager, M., Antonini, F., Vigl, L., 1995. Evinos-Mornos tunnel — Greece construction of a 30 km long hydraulic tunnel in less than three years under the most adverse geological conditions. Rapid Excavation and Tunnelling Conference, San Francisco. SME Inc., Littleton, pp. 747–767 (Chapter 47).

Guglielmetti, V., Grasso, P., Mahtab, A., Xu, S. (Eds.), 2008. Mechanized Tunnelling in Urban Areas, Design Methodology and Construction Control. Taylor & Francis Group, London.

Haslett, S.K., 2000. Coastal Systems. Routledge, London.

Julivert, M., Duran, H., 1990. Paleozoic stratigraphy of the Central and Northern part of the Catalonian Coastal ranges (NE Spain). Acta Geol. Hisp. 25 (1–2), 3–12.

Kolic, D., Bai, Y., Nicolas, A., 2009. TBM tunnelling in karst regions: Wanjiazhai Project. In: Vrkljan, I. (Ed.), Rock Engineering in Difficult Ground Conditions — Soft Rocks and Karst. ISRM Sponsored Regional Symposium, Croatia (6 pp.).

Kovári, K., Ramoni, M., 2006. Urban tunnelling in soft ground using TBMs. Tunneling and Trenchless Technology in the 21st CenturyInternational conference and exhibition on tunnelling and trenchless technology, Subang Jaya – Selangor Darul Ehsan. The Institution of Engineering, Malaysia, pp. 17–31.

Lang, M.A., 2014. TMB Hyperbaric Intervention: to Intervene or not to Intervene. TBM: Tunnel Business Magazine, pp. 32–34 (June).

Llopis-Lladó, N., 1942. Los terrenos cuaternarios del llano de Barcelona. Publ. Instituto Geológico-Topográfico de la Diputación Provincial de Barcelona VI, pp. 5–52.

Ma, H.S., Wang, J., 2014. TBM tunneling in squeezing ground: problems and solutions. In: He, X., Mitri, H., Nie, B., Wang, Y., Ren, T.X., Chen, W., Li, X. (Eds.), Progress in Mine Safety Science and Engineering II. Taylor and Francis Group, London, pp. 339–345.

Maidl, B., Herrenknecht, M., Anheuser, L., 1996. Mechanised Shield Tunnelling. Ernst & Sohn, Berlin.

Marchionni, V., Guglielmetti, V., 2007. EPB-tunnelling control and monitoring in a urban environment: the experience of the "Nodo in Bologna" construction (Italian High Speed Railway system). In: Barták, Hrdina, Romancov, Zlámal (Eds.), Underground Space — The 4th Dimension of Metropolises. Taylor & Francis Group, London, pp. 895–901.

Marqués, M.A., 1984. Les formacions quaternàries del delta del Llobregat. Institut d'Estudis Catalans, Barcelona.

Martí, D., Carbonell, R., Flecha, I., Palomares, I., Font-Capó, J., Vázquez-Suñé, E., Pérez-Estaún, A., 2008. Case history. High-resolution seismic characterization in an urban area: subway tunnel construction in Barcelona, Spain. Geophysics 73-2, B41–B50.

Mignini, A., Orfila, T., Colomer, M., Bertagnolio, F., 2008. Surface settlement minimization in soft soil when excavating with an Earth Pressure Balance shield. Barcelona Metro Line 9 Mas Blau — San Cosme station. Tunnelling working procedure. In: Alonso, E., Arroyo, M. (Eds.), Jornadas Técnicas de túneles con EPB. Simulación y Control de la Tuneladora, Barcelona, pp. 149–162.

Orfila, T., Moyà, N., Della Valle, N., 2007. Optimising Line 9's EPBM Parameters. Tunnels and Tunnelling International, pp. 40–45 (April).

Parcerisa, D., Thiry, M., Gómez-Gras, D., Calvet, F., 2001. Proposition d'un modèle de silicification superficielle des grès néogènes de Montjuïc, Barcelone (Espagne): paragenèse minérales, environnements géochimiques et circulation des fluides. Bull. Soc. Geol. Fr. 172, 751–764.

Ramoni, M., Anagnostou, G., 2010. Tunnel boring machines under squeezing conditions. Tunn. Undergr. Space Technol. 25, 139–157.

Riba, O., Colombo, F., 2009. Barcelona: la Ciutat Vella i el Poblenou. Assaig de geologia urbana. Institut d'Estudis Catalans, Barcelona.

Salvany, J.M., 2013. Anàlisis y correlación de sondeos mecánicos en los depósitos miocenos de Montjuïc (Barcelona): implicaciones estructurales. Estud. Geol. 69 (2), 149–171.

Santanach, P., Casas, J.M., Gratacós, O., Liesa, M., Muñoz, J.A., Sàbat, F., 2011. Variscan and Alpine structure of the hills of Barcelona: geology in an urban area. J. Iber. Geol. 37 (2), 121–136.

Schwarz, H., Boté, R., Gens, A., 2006. Construction of a new Metro line in Barcelona: design criteria, excavation and monitoring. Geotechnical Aspects of Underground Construction in Soft Ground. Taylor & Francis Group, Rotterdam, pp. 757–762.

Shahriar, K., Rostami, J., Hamidi, J.K., 2009. TBM tunnelling and analysis of high emission accident in Zagros long tunnel. ITA-AITES World Tunnel Congress and 35th ITA-AITES General Assembly, Budapest, Hungary (9 pp.).

Shang, Y., Xue, J., Wang, S., Yang, Z., Yang, J., 2004. A case history of Tunnel Boring Machine jamming in an inter-layer shear zone at the Yellow River Diversion Project in China. Eng. Geol. 71, 199–211.

Solé-Sabarís, L., 1963. Ensayo de interpretación del Cuaternario barcelonés. Misc. Barcinonensia 3, 7–54.

Tseng, D.J., Tsai, B.R., Chang, L.C., 2001. A case study ground treatment for a rock tunnel with high groundwater ingression in Taiwan. Tunn. Undergr. Space Technol. 16, 175–183.

Velasco, V., Cabello, P., Vázquez-Suñé, E., López-Blanco, M., Ramos, E., Tubau, I., 2012. A sequence stratigraphic based geological model for constraining hydrogeological modeling in the urbanizad area of the Quaternary Besòs delta (NW Mediterranean coast, Spain). Geol. Acta 10 (4), 373–393.

Vicente, J., 1986. El Pliocè marí del pla de Barcelona i del delta del Besòs. Butlletí Centre d'Estudis de la Natura de Barcelona Nord 2, pp. 52–60.

Warner, J., 2004. Practical Handbook of Grouting, Soil Rock and Structures. John Wiley & Sons, Hoboken.

Wenner, D., Wannenmacher, H., 2009. Alborz Service Tunnel in Iran: TBM tunnelling in difficult ground conditions and its solutions. 1st Regional and 8th Iranian Tunneling Conference, Tehran (12 pp.).

Zarei, H.R., Uromoihy, A., Sharifzadeh, M., 2012. Identifying geological hazards related to tunnelling in carbonate karstic rocks — Zagros, Iran. Arab. J. Geosci. 5 (3), 457–464.

Zuloaga, I., 2004. Superjet-grouting nueva tecnología para la mejora in situ del terreno. Jornadas Técnicas SEMSIG-AETESS. 4ª Sesión, mejora del terreno mediante inyecciones y Jet-Grouting. CEDEX, Madrid (16 pp.).